

# Electric-field-induced current-voltage characteristics in electronic conducting perovskite thin films

Cite as: Appl. Phys. Lett. **100**, 012101 (2012); <https://doi.org/10.1063/1.3663529>

Submitted: 12 August 2011 . Accepted: 27 September 2011 . Published Online: 03 January 2012

Jennifer L. M. Rupp, Patrick Reinhard, Daniele Pergolesi, Thomas Ryll, Rene Tölke, and Enrico Traversa



View Online



Export Citation

## ARTICLES YOU MAY BE INTERESTED IN

[Unusual defect physics in  \$\text{CH}\_3\text{NH}\_3\text{PbI}\_3\$  perovskite solar cell absorber](#)

Applied Physics Letters **104**, 063903 (2014); <https://doi.org/10.1063/1.4864778>

[Defect density and dielectric constant in perovskite solar cells](#)

Applied Physics Letters **105**, 153502 (2014); <https://doi.org/10.1063/1.4897329>

[Mechanisms for light induced degradation in  \$\text{MAPbI}\_3\$  perovskite thin films and solar cells](#)

Applied Physics Letters **109**, 233905 (2016); <https://doi.org/10.1063/1.4967840>

## Lock-in Amplifiers up to 600 MHz

starting at

\$6,210



Zurich Instruments

Watch the Video

## Electric-field-induced current-voltage characteristics in electronic conducting perovskite thin films

Jennifer L. M. Rupp,<sup>1,a)</sup> Patrick Reinhard,<sup>1</sup> Daniele Pergolesi,<sup>1</sup> Thomas Ryll,<sup>2</sup> Rene Tölke,<sup>2</sup> and Enrico Traversa<sup>1</sup>

<sup>1</sup>National Institute for Material Science (NIMS), 1-1 Namiki, Tsukuba, Ibaraki 305-0044, Japan

<sup>2</sup>Department of Materials, ETH Zurich, Wolfgang-Pauli-Str.10, CH-8093 Zurich, Switzerland

(Received 12 August 2011; accepted 27 September 2011; published online 3 January 2012)

Mixed ionic-electronic conductors (MIECs) such as the (La,Sr)(Co,Fe)O<sub>3-d</sub> perovskite family are well described in their charge transport through their high temperature applications, i.e., as solid-oxide fuel cell electrodes (600–1000 °C). In this study, the current-voltage (*I-V*) profiles of these well-known MIEC perovskites are studied between room temperature and 150 °C under bias of ±15 V for potential applications in resistance random access memories. The impact of the metal-oxide interface on the *I-V* characteristics ranging from ohmic to non-linear hysteretic is discussed for metals of varying work functions and redox potentials, as well as changes in metal electrode distances and areas. © 2012 American Institute of Physics. [doi:10.1063/1.3663529]

Mixed ionic-electronic conductors (MIECs) such as ABO<sub>3</sub> perovskite oxides are ideal model systems to study charge transport characteristics, and their impact on the material's current-voltage (*I-V*) profiles under bias. In general, the charged defects of MIEC perovskites are of two kinds: oxygen vacancies, which are donors in this case, and electronic charge carriers, being either electrons (n-type) or holes (p-type). The concentration of these defects can be changed systematically by (1) the generation of *intrinsic defects* by modification of temperature or oxygen partial pressure, resulting in a change of the redox-potential of the perovskite or (2) the generation of *extrinsic defects* by doping of both the A and B sites of the perovskite with cations of modified ionic radii and valence state.<sup>1</sup> The perovskite material system (La,Sr)(Co,Fe)O<sub>3-d</sub> (LSCF) is a well known MIEC used in high temperature solid state electrochemistry applications<sup>2</sup> such as in solid oxide fuel cell cathodes<sup>3</sup> or oxygen permeation membranes.<sup>4</sup> In this case, they are predominantly p-type (hole) conductors with an ionic conductivity contribution.<sup>5</sup> Recently, there is interest to study the *I-V* characteristics of MIECs under bias potential at room temperature for possible applications as alternative oxide materials in future non-volatile resistance random access memories (RRAMs).<sup>6,7</sup> Such devices consist of a metal-oxide-metal capacitor-like structure which is non-linearly switched between a high and low resistance through a bias voltage at room temperature. These reveal faster switching capabilities (nano-seconds) and lower steering voltages (mV) compared to state-of-the-art Flash or RAM memories.<sup>7</sup> Commonly, titania or perovskites-based on manganates ((Pr,Ca)MnO<sub>3</sub>) or titanates (SrTiO<sub>3</sub>,BaTiO<sub>3</sub>) are considered. It is suggested to investigate as case examples the *I-V* profiles of the MIEC (La,Sr)(Co,Fe)O<sub>3-d</sub> under bias.

La<sub>0.6</sub>Sr<sub>0.4</sub>Co<sub>0.2</sub>Fe<sub>0.8</sub>O<sub>3-x</sub> was deposited by pulsed laser deposition (PLD) at 600 °C, according to Ref. 8, yielding polycrystalline thin films 300-500 nm thick. An array of up

to 72 metal electrode pairs (Pt, Au, Ag, or Ta) was microfabricated on top of the film. The metal electrode separation varied between 10–170 μm, and the electrode quadratic areas from 400<sup>2</sup> μm<sup>2</sup> to 600<sup>2</sup> μm<sup>2</sup>. A cross-sectional view of the sample geometry is shown in Fig. 1(a) for a single electrode pair. Metal films were sputtered by DC magnetron sputtering in 1–20 mTorr of Ar (purity >99.998%), at 205-360 W and at room temperature. The electrodes were microstructured see Refs. 8 and 9 for details. In-plane *I-V* measurements were registered with a Solatron (1260 impedance analyzer), where the metal electrodes were contacted with Cu-Be needle tips.

High resolution images of a microfabricated Ag-electrode test-structure on a La<sub>0.6</sub>Sr<sub>0.4</sub>Co<sub>0.2</sub>Fe<sub>0.8</sub>O<sub>3-x</sub> PLD film is shown in Fig. 1(b). The perovskite films revealed an isotropic polycrystalline microstructure with grains approximately 10 nm in size on average. XRD studies confirmed the cubic perovskite phase for the La<sub>0.6</sub>Sr<sub>0.4</sub>Co<sub>0.2</sub>Fe<sub>0.8</sub>O<sub>3-x</sub> PLD film, see details in Ref. 10. Metal electrodes with a precision of ±1 μm in feature size were structured on top of the oxide film, which allowed for *I-V* measurements of defined electrode distances from 170-to-10 μm for in-plane geometries.

*I-V* characteristics as a function of the metal electrode material and sweep rate are presented for the La<sub>0.6</sub>Sr<sub>0.4</sub>Co<sub>0.2</sub>Fe<sub>0.8</sub>O<sub>3-x</sub> films for equal electrode separation of 70(1) μm in Fig. 2. Literature reports that the work function of the following electrode materials decreases in the following fashion: Pt → Au → Ag → Ta, i.e., from Figs. 2(a)–2(c), see Table I. A work function of approximately 5.6(3) eV is reported for La<sub>1</sub>Sr<sub>1-x</sub>CoO<sub>3-x</sub> perovskites in the literature.<sup>11</sup> Consequently, the work function difference is almost zero for Pt electrodes on the oxide film and increased to Δ1.2 eV when Ta electrodes were used on the oxide film, Table I. Decreasing the work function of the metal electrodes from Pt to Ta results in a transition from (almost) ohmic to non-linear *I-V* characteristics. The choice of electrode material affects the *I-V* profiles of the biased films. Where a small difference in the work function existed between La<sub>0.6</sub>Sr<sub>0.4</sub>Co<sub>0.2</sub>Fe<sub>0.8</sub>O<sub>3-x</sub> and the metal electrode, an almost ohmic response was measured by a linear *I-V* characteristic,

<sup>a)</sup>Present address: Department of Material Science and Engineering and Nuclear Science and Engineering, Massachusetts Institute of Technology (MIT), Cambridge, Massachusetts 02139, USA. Electronic mail: jrupp@mit.edu.

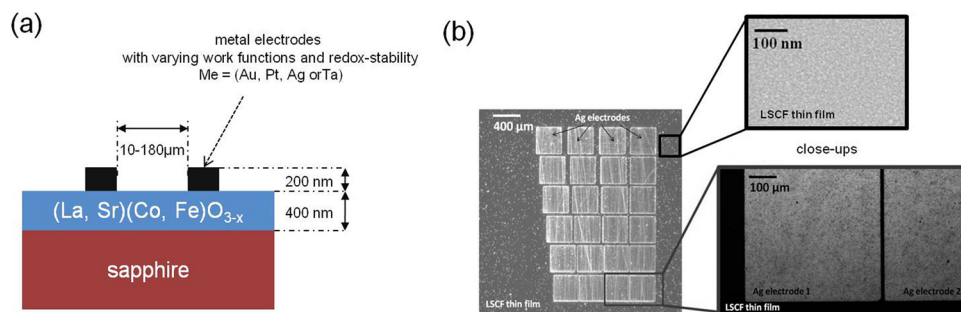


FIG. 1. (Color online) (a) Schematic cross-section of the microstructured top-contacts to measure the current-voltage ( $I$ - $V$ ) profiles of a MIEC perovskite  $(\text{La,Sr})(\text{Co,Fe})\text{O}_{3-x}$  films. The metal electrode material is systematically changed in their distance, area, as well as their work function, and redox potential towards the oxide. (b) Light microscopy and SEM in-plane views of different parts of the measuring structure. The full array structure with varying electrode distances between 10-170(1)  $\mu\text{m}$  is shown in the given example for microfabricated Ag electrodes. Close-ups display two electrodes at 10(1)  $\mu\text{m}$  distance on the  $\text{La}_{0.6}\text{Sr}_{0.4}\text{Co}_{0.2}\text{Fe}_{0.8}\text{O}_{3-d}$  perovskite film, and a SEM close up of the  $\text{La}_{0.6}\text{Sr}_{0.4}\text{Co}_{0.2}\text{Fe}_{0.8}\text{O}_{3-d}$  perovskite film microstructure. The mixed ionic-electronic conducting film was processed by PLD, whereas electrodes were sputtered and structured via microfabrication.

under bias. Metals that are inert to oxygen such as Au, along with metals that react to oxygen such as Ta and Ag, showed non-linear  $I$ - $V$  characteristics in this study. To study the impact of charge carrier redistribution under bias, the samples were subjected to different sweep rates changing from 0.2 to 10 mV/s. The hysteresis of the  $I$ - $V$  characteristics increased for all tested electrodes whilst decreasing the sweep rate to 0.2 mV/s, which reflects the strong time-dependence. As a second experiment, the temperature-dependent  $I$ - $V$  measurements were performed to actively change the intrinsic defects of the MIEC perovskite in a biased state with a 10 mV/s sweep rate, Fig. 3. The *ohmic IV-profiles* of the Pt metals on the MIEC oxide remain temperature independent in the case of zero difference in work function. *Non-linear I-V hysteresis* pronounces with temperature increase from room temperature to 150 °C, as well as with increasing work function difference between the metal and the MIEC oxide.

The activation energies associated with the resistivity were calculated using the Arrhenius equation and were around 0.14(4) eV over the temperature range of 20–150 °C and  $\pm 1$ –10 V. The activation energy is found to be independent of the electrode material choice. The reported activation energy under non-linear transport is in agreements with those of bulk and thin film<sup>3</sup>  $\text{La}_{0.6}\text{Sr}_{0.4}\text{Co}_{0.2}\text{Fe}_{0.8}\text{O}_{3-x}$  electrodes in the field of fuel cell and oxygen separation membranes, in which a maximum of 1 V (Nernst voltage) is present during testing at 600–1000 °C. The rather low activation energy of this MIEC oxide is discussed in high temperature literature as a predominant hole conductivity by small polaron hopping over ionic conductivity.<sup>12</sup> It is further reported from partial pressure dependent measurements that the major charge transfer is hole

conduction compared to the ionic contribution of the MIEC for these rather low temperatures in air.<sup>5</sup> Since we report a comparable activation energy of conductivity for the bias-dependent measurements between room temperature and 150 °C it is reasonable to assume that the predominant charge transfer of the MIEC oxide occurs by hole conduction for the reported  $I$ - $V$  profiles when biased up to  $\pm 10$  V.

Three conclusions may be drawn from this work. First, mixed ionic-electronic conducting perovskites of the material

TABLE I. Literature comparison of work functions of the metal electrode materials Pt, Au, Ag, and Ta relative to the one of the oxide  $\text{La}_{1-x}\text{Sr}_x\text{CoO}_{3-d}$ .

Material	Work function (eV)	Ref.
$\text{La}_{1-x}\text{Sr}_x\text{CoO}_{3-d}$	4.8–5.1	11
Pt	5.3–5.9	14 and 15
Au	5.1–5.5	14
Ag	4.5–4.7	14
Ta	4.1–4.8	14 and 15

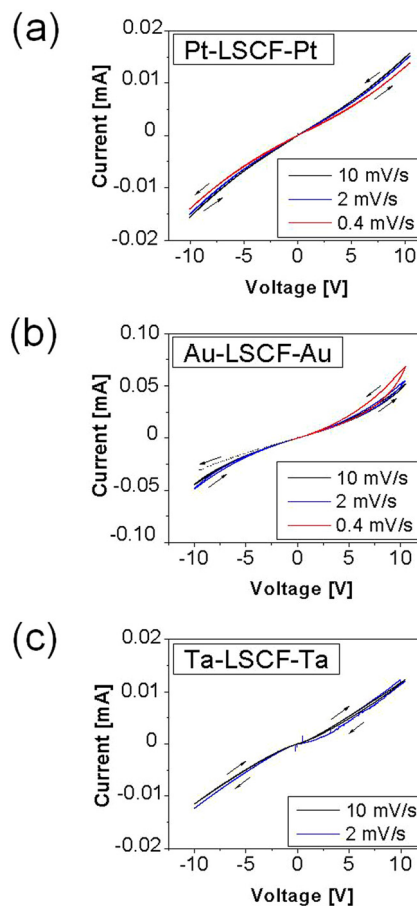


FIG. 2. (Color online) Sweep-rate dependent  $I$ - $V$  characteristics of a  $\text{La}_{0.6}\text{Sr}_{0.4}\text{Co}_{0.2}\text{Fe}_{0.8}\text{O}_{3-d}$  mixed ionic-electronic oxide with respect to metal electrode material. (a) Pt-LSCF-Pt, (b) Au-LSCF-Au, and (c) Ta-LSCF-Ta.  $I$ - $V$  characteristics were recorded for in-plane electrode contacts separated by 70(1)  $\mu\text{m}$  at room temperature.

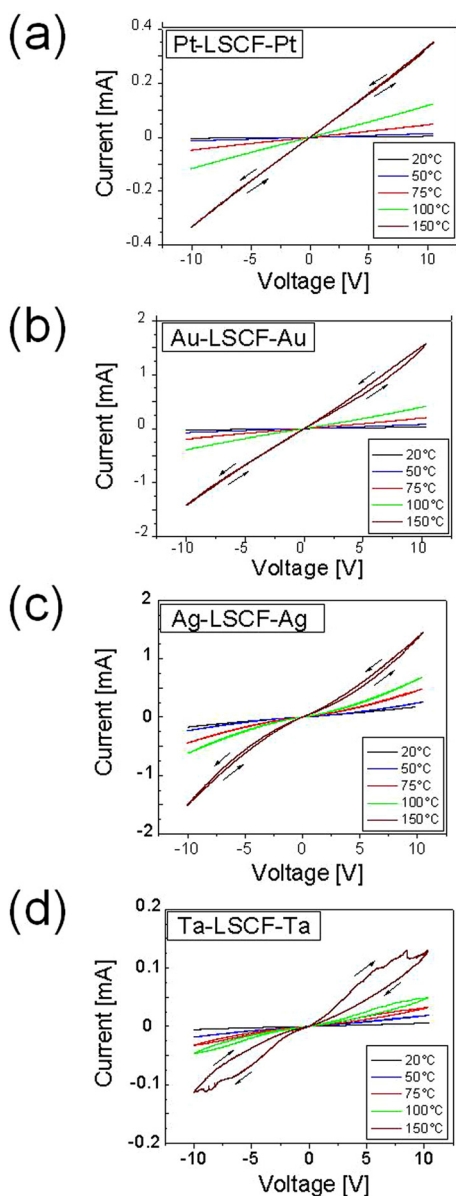


FIG. 3. (Color online) Temperature-dependent  $I$ - $V$  characteristics of a  $\text{La}_{0.6}\text{Sr}_{0.4}\text{Co}_{0.2}\text{Fe}_{0.8}\text{O}_{3-d}$  mixed ionic-electronic oxide with respect to metal electrode material. (a) Pt-LSCF-Pt, (b) Au-LSCF-Au, (c) Ag-LSCF-Ag, and (d) Ta-LSCF-Ta.  $I$ - $V$  characteristics were recorded at 10 mV/s for in-plane electrode contacts separated by  $10(1) \mu\text{m}$ .

system  $(\text{La,Sr})(\text{Co,Fe})\text{O}_{3-d}$  are suitable to show the full range of behaviour from ohmic to non-linear  $I$ - $V$  characteristics. The choice in metal material affects the charge transport at the oxide-metal interface. It is reported that for low work function differences between the oxide and metal and larger electrode distances, purely ohmic  $I$ - $V$  profiles are determined. A work function difference of at least  $\Delta 0.3 \text{ eV}$  between the perovskite and the metal electrode were measured to result in changes of the  $I$ - $V$  characteristics to non-linear.

Recent computational work of Riess and co-workers highlighted the importance to decrease the overall metal

electrode distance to 100 nm or lower to probe MIEC oxides.<sup>13</sup> Thereby, the metal-oxide interface charge transfer contribution becomes more dominant, and stronger hysteresis in the  $I$ - $V$  profiles is observable. We confirm these trends experimentally.

Second, this perovskite group is of potential as a model system to gain understanding on charge transport under bias. The role of ionic and electronic charge carriers can be clarified through controlled intrinsic and extrinsic doping experiments. In this study, intrinsic doping was changed through temperature increase, indicating a predominant hole and minor ionic conduction mechanism active during the ohmic and non-linear  $I$ - $V$  profile under bias. This is supported by the activation energy of conductivity which remains around 0.14 eV independent on the metal electrode material choice, applied bias, or heating from room temperature to 150 °C. The measured activation energy agrees well with literature on high-temperature conduction measurements of non-biased  $\text{La}_{0.6}\text{Sr}_{0.4}\text{Co}_{0.2}\text{Fe}_{0.8}\text{O}_{3-x}$  bulk and thin films.

Third, oxidation and reduction of the metal film under bias were not confirmed to be a prime cause for the non-linear  $I$ - $V$  profile in the perovskite  $\text{La}_{0.6}\text{Sr}_{0.4}\text{Co}_{0.2}\text{Fe}_{0.8}\text{O}_{3-x}$  used in this work. It is reasonable to assume that the valence states of the oxide change locally under the applied bias leading to accumulation and depletion zones of charge carriers in the vicinity close to the metal electrodes.

Professor H. Tuller from Massachusetts Institute of Technology (MIT) is thanked for stimulating discussion. The Swiss National Research Foundation (SNF) is acknowledged for the fellowship PA00P2-134153.

<sup>1</sup>K. Kamata, T. Nakamura, and T. Sata, *Bull. Tokyo Inst. Technol.* **120**, 73 (1974).

<sup>2</sup>F. S. Baumann, J. Fleig, H. U. Habermeier, and J. Maier, *Solid State Ionics* **177**(11–12), 1071 (2006).

<sup>3</sup>D. Beckel, U. P. Muecke, T. Gyger, G. Florey, A. Infortuna, and L. J. Gauckler, *Solid State Ionics* **178**(5–6), 407 (2007).

<sup>4</sup>B. T. Dalslet, M. Sogaard, and P. V. Hendriksen, *Solid State Ionics* **180**(17–19), 1050 (2009).

<sup>5</sup>E. Bucher and W. Sitte, *J. Electroceram.* **13**(1–3), 779 (2004).

<sup>6</sup>R. Waser, R. Dittmann, G. Saikov, and K. Szot, *Adv. Mater.* **21**, 2632 (2009).

<sup>7</sup>H. Akinaga, H. Shima, F. Takano, I. H. Inoue, and H. Takagi, *IEEJ Trans. Electr. Electron. Eng.* **2**(4), 453 (2007).

<sup>8</sup>N. J. Simrick, J. A. Kilner, A. Atkinson, J. L. M. Rupp, T. M. Ryll, A. Bieberle-Hütter, H. Galinski, and L. J. Gauckler, *Solid State Ionics* **192**(1), 619 (2011).

<sup>9</sup>T. Ryll, J. L. M. Rupp, A. Bieberle-Hütter, H. Galinski, and L. J. Gauckler, *Scr. Mater.* **65**(2), 84 (2011).

<sup>10</sup>D. Beckel, A. Dubach, A. N. Grundy, A. Infortuna, and L. J. Gauckler, *J. Eur. Ceram. Soc.* **28**(1), 49 (2008).

<sup>11</sup>K. Kiyokawa, K. Sugiyama, M. Tomimatsu, H. Kurokawa, and H. Miura, *Thin Solid Films* **386**(2), 147 (2001).

<sup>12</sup>H. Ullmann, N. Trofimenko, F. Tietz, D. Stover, and A. Ahmad-Khanlou, *Solid State Ionics* **138**(1–2), 79 (2000).

<sup>13</sup>A. Leshem, E. Gonen, and I. Riess, *Nanotechnology* **22**(25), 254024 (2011).

<sup>14</sup>R. C. Weast, *CRC Handbook of Chemistry and Physics* (CRC, Boca Raton, FL, 2008), pp. 12–114.

<sup>15</sup>H. Kawano, *Appl. Surf. Sci.* **254**(22), 7187 (2008).